

Higher-order contributions to the Rashba-Bychkov effect with application to the Bi/Ag(111) surface alloy

Sz. Vajna,¹ E. Simon,^{1,2} A. Szilva,¹ K. Palotas,¹ B. Ujfalussy,³ and L. Szunyogh^{1,*}

¹*Department of Theoretical Physics, Budapest University of Technology and Economics, Budafoki út 8, H-1111 Budapest, Hungary*

²*Loránd Eötvös University, Department of Physics, POB 32, H-1518 Budapest, Hungary*

³*Institute for Solid State Physics and Optics, Wigner Research Centre for Physics, Hungarian Academy of Sciences, PO Box 49, H-1525 Budapest, Hungary*

(Received 18 October 2011; revised manuscript received 6 January 2012; published 6 February 2012)

In order to explain the anisotropic Rashba-Bychkov effect observed in several metallic-surface-state systems, we use $k \cdot p$ perturbation theory with a simple group-theoretical analysis and construct effective Rashba Hamiltonians for different point groups up to third order in the wave number. We perform relativistic *ab initio* calculations for the $(\sqrt{3} \times \sqrt{3})R30^\circ$ Bi/Ag(111) surface alloy, and from the calculated splitting of the band dispersion we find evidence of the predicted third-order terms. Furthermore, we derive expressions for the corresponding third-order Rashba parameters to provide a simple explanation of the qualitative difference concerning the Rashba-Bychkov splitting of the surface states at Au(111) and Bi/Ag(111).

DOI: [10.1103/PhysRevB.85.075404](https://doi.org/10.1103/PhysRevB.85.075404)

PACS number(s): 71.15.Rf, 73.20.At, 75.70.Tj

I. INTRODUCTION

Since the first experimental verification by LaShell *et al.*,¹ the spin-orbit-induced splitting of Shockley states on metallic surfaces called the Rashba-Bychkov (RB) effect² gained focus of experimental and theoretical research. These investigations range from the prototypical L -gap surface states at Au(111) and Ag(111)^{3–7} and also at Au(110),^{8–10} through Li/W(110) and Li/Mo(110) overlayers¹¹ and the Gd(0001) surface,¹² to a large number of metallic surfaces and surface alloys related to Bi, Pb, or Sb where the $5p$ and $6p$ orbitals show a pronounced spin-orbit splitting.^{13–28} This huge interest is mainly triggered by potential spintronics applications in relation to the Datta-Das transistor,²⁹ the spin Hall effect,³⁰ and the anomalous Hall effect.³¹

While accurate *ab initio* calculations satisfactorily account for most features of the measured dispersion relations of metallic surface states, there is an obvious need to explain the RB effect in terms of simple models containing a few, easily identifiable parameters. The simplest effective Hamiltonian of a two-dimensional electron gas, subject to spin-orbit interaction (SOI), includes in addition to the kinetic energy $\varepsilon_0 + \frac{\hbar^2 \mathbf{k}^2}{2m^*}$ (\mathbf{k} and m^* being the wave vector and the effective mass of the electrons, respectively), a Rashba term:^{2,32}

$$H_R(\mathbf{k}) = \alpha_R(k_x \sigma_y - k_y \sigma_x), \quad (1)$$

where α_R is the so-called Rashba parameter and σ_i ($i = x, y, z$) denote the Pauli matrices. The corresponding eigenvalues, $\varepsilon_{\pm}(\mathbf{k}) = \varepsilon_0 + \frac{\hbar^2 \mathbf{k}^2}{2m^*} \pm \alpha_R k$ ($k = |\mathbf{k}|$), show an isotropic splitting for $\mathbf{k} \neq 0$, and at least for moderate values of k , they readily can be fit to most experimental and *ab initio* dispersion relations.

Although not yet detected experimentally,⁸ an RB splitting that is anisotropic in k space is obvious for the surface states at Au(110). The C_{2v} point-group symmetry³³ of the system not only implies an anisotropy of the effective mass, $m_x^* \neq m_y^*$, but, as discussed in terms of $k \cdot p$ perturbation theory,^{10,35} it leads to a Rashba Hamiltonian containing two independent

Rashba parameters, α_R^1 and α_R^2 :

$$H_R(\mathbf{k}) = \alpha_R^1 k_x \sigma_y + \alpha_R^2 k_y \sigma_x. \quad (2)$$

Fully relativistic *ab initio* calculations confirmed the existence of the anisotropic RB splitting at Au(110),⁹ matching with a high accuracy to the eigenvalues of the effective Hamiltonian in Eq. (2).¹⁰

Even in the case of high-symmetry surfaces, i.e., having a point group of C_{3v} or C_{4v} , several studies^{13,15,18,24,26,27} called attention to an anisotropic RB splitting. In Ref. 34 the anisotropic RB effect at Bi/Ag(111) and Pb/Ag(111) surfaces was reproduced by using a nearly-free electron model and explained due to in-plane structural inversion asymmetry. From the group-theoretical analysis in Ref. 35 it is, however, clear that under C_{3v} and C_{4v} point-group symmetry an effective 2×2 Hamiltonian that is linear in the components of \mathbf{k} must be of the form of Eq. (1); hence it cannot explain the observed anisotropy of the RB splitting. Thus we conclude that in these systems the anisotropic RB effect can be described by a Hamiltonian containing at least third-order polynomials of k_x and k_y . It should be noted that the second-order terms are related to the kinetic energy (effective mass terms) that are irrelevant to the RB splitting.

To construct Rashba Hamiltonians up to third order in k , in the present work we use $k \cdot p$ perturbation theory and group-theoretical methods different from Ref. 35. Our analysis of the effective Hamiltonian is closely related to that of Ref. 36, where, for the case of C_{3v} symmetry, the correct form of $H(\mathbf{k})$ is derived up to third order in k and the corresponding band dispersion was used to explain the hexagonal warping of the surface states' Fermi contour observed experimentally in the topological insulator Bi₂Te₃.³⁷ A unified phenomenological description of anisotropy effects on the Rashba and the topological insulator surface states under C_{3v} symmetry has recently been exploited based on such an effective Hamiltonian.³⁸

We also perform relativistic *ab initio* calculation for the Bi/Ag(111) ordered alloy in $(\sqrt{3} \times \sqrt{3})R30^\circ$ superstructure and confirm that for higher values of k , but still in the measured

range, third-order terms of the Rashba Hamiltonian are needed to reproduce the RB splitting and that these terms are of the predicted form. Moreover, using explicit expressions of the third-order Rashba parameters within $k \cdot p$ perturbation theory and calculated spectral densities at the Brillouin zone center we are able to give a simple explanation of why the Au(111) and the Bi/Ag(111) surface states exhibit isotropic and anisotropic RB splitting, respectively.

II. PERTURBATION THEORY AND SYMMETRY ANALYSIS

Let \mathbf{Q} be a high-symmetry point of the surface Brillouin zone (SBZ), for which a pair of spin-degenerate eigenstates exists on a nonmagnetic surface. Due to time reversal symmetry, this is always the case if $\mathbf{Q} = -\mathbf{Q} + \mathbf{K}$ is satisfied, where \mathbf{K} is a two-dimensional (2D) reciprocal-lattice vector. Such points are the center of the SBZ ($\bar{\Gamma}$) and some special points at the boundary of SBZ, such as the \bar{X} , \bar{Y} , and \bar{S} points for a primitive rectangular lattice, the \bar{M} and \bar{X} points for a square lattice, and the \bar{M} point for a hexagonal lattice. Regarding what follows, our investigations will concern solely this case termed as the proper Rashba effect.⁹ As pointed out in Ref. 9, due to double-group symmetry degeneracy can happen at points of the SBZ that don't meet the above condition, like the \bar{K} point for a hexagonal lattice (improper Rashba effect).

To describe the surface band around \mathbf{Q} it is worth to label the corresponding Bloch states by the wave number with respect to \mathbf{Q} , $\psi_{\mathbf{Q}+\mathbf{k}}$, and introduce a new wave function $\phi_{\mathbf{k}}$ as

$$\psi_{\mathbf{Q}+\mathbf{k}}(\mathbf{r}) = e^{i\mathbf{k}\mathbf{r}} \phi_{\mathbf{k}}(\mathbf{r}), \quad (3)$$

with the boundary condition $\phi_{\mathbf{k}}(\mathbf{r} + \mathbf{T}) = e^{i\mathbf{Q}\mathbf{T}} \phi_{\mathbf{k}}(\mathbf{r})$, where \mathbf{T} is a 2D real-lattice vector. Considering the Hamilton operator $\mathcal{H} = \frac{\mathbf{p}^2}{2m} + V + \mathcal{H}_{\text{SO}}$, with the crystal potential V and \mathcal{H}_{SO} denoting the spin-orbit interaction,

$$\mathcal{H}_{\text{SO}} = \frac{\hbar}{4m^2c^2} (\nabla V \times \mathbf{p}) \cdot \boldsymbol{\sigma}, \quad (4)$$

and the wave functions $\phi_{\mathbf{k}}$ satisfy the eigenvalue equation

$$[\mathcal{H}_0(\mathbf{k}) + \mathcal{H}_{\text{SO}}(\mathbf{k})] \phi_{\mathbf{k}} = \varepsilon(\mathbf{k}) \phi_{\mathbf{k}} \quad (5)$$

with

$$\mathcal{H}_0(\mathbf{k}) = \frac{(\hbar\mathbf{k} + \mathbf{p})^2}{2m} + V, \quad (6)$$

and

$$\mathcal{H}_{\text{SO}}(\mathbf{k}) = \frac{\hbar}{4m^2c^2} [\nabla V \times (\hbar\mathbf{k} + \mathbf{p})] \cdot \boldsymbol{\sigma}. \quad (7)$$

Following the recipe used in Ref. 10, in the first step we look for the solution of the Schrödinger equation,

$$\mathcal{H}_0(\mathbf{k})\phi_{\mathbf{k}}^0 = \varepsilon_0(\mathbf{k})\phi_{\mathbf{k}}^0, \quad (8)$$

which can be elucidated, e.g., in terms of $k \cdot p$ perturbation theory. Although such a calculation provides deeper insight into the problem,¹⁰ in this section we just make use of the symmetry properties of the solutions, $\varepsilon_0(\mathbf{k})$ and $\phi_{\mathbf{k}}^0$. First we note that since $\mathcal{H}_0(\mathbf{k})$ is independent of the spin, the solutions of Eq. (8) remain degenerate in spin space. Time

reversal symmetry, $T\mathcal{H}_0(\mathbf{k})T^{-1} = \mathcal{H}_0(-\mathbf{k})$ with $T\psi = \psi^*$, then immediately implies

$$\varepsilon_0(-\mathbf{k}) = \varepsilon_0(\mathbf{k}), \quad (9)$$

$$\phi_{-\mathbf{k}}^0 = (\phi_{\mathbf{k}}^0)^*, \quad (10)$$

where the phase of $\phi_{\mathbf{k}}^0$ has been fixed without loss of generality. Clearly from Eq. (9), a polynomial form of $\varepsilon_0(\mathbf{k})$ contains only even powers; the first nontrivial (second-order) terms are obviously related to the effective masses.

We can draw further relations from point-group symmetry. Let $G_{\mathbf{Q}}$ be the small group of \mathbf{Q} , i.e., $g\mathbf{Q} = \mathbf{Q} + \mathbf{K}$ for any $g \in G_{\mathbf{Q}}$, and \mathbf{K} denoting an appropriate reciprocal-lattice vector. Using the standard definition for the action of a symmetry operation, $(g \circ f)(\mathbf{r}) = f(g^{-1}\mathbf{r})$, from the symmetry of the Hamilton operator, $g \circ \mathcal{H}_0(\mathbf{k}) = \mathcal{H}_0(g\mathbf{k})$, one easily can derive

$$\varepsilon_0(g\mathbf{k}) = \varepsilon_0(\mathbf{k}), \quad (11)$$

$$g \circ \phi_{\mathbf{k}}^0 = \phi_{g\mathbf{k}}^0. \quad (12)$$

In the second step, using $\mathcal{H}_{\text{SO}}(\mathbf{k})$ as perturbation and $\phi_{\mathbf{k}}^0 \chi_s$ with χ_s being spin eigenfunctions ($s = \pm \frac{1}{2}$) as unperturbed wave functions, first-order degenerate perturbation theory is applied. The Rashba Hamiltonian $H_R(\mathbf{k})$ is defined as the corresponding 2×2 matrix,

$$H_R(\mathbf{k}) = \boldsymbol{\alpha}(\mathbf{k}) \cdot \boldsymbol{\sigma}, \quad (13)$$

where

$$\boldsymbol{\alpha}(\mathbf{k}) = \langle \phi_{\mathbf{k}}^0 | \frac{\hbar}{4m^2c^2} (\nabla V \times (\hbar\mathbf{k} + \mathbf{p})) | \phi_{\mathbf{k}}^0 \rangle. \quad (14)$$

Our present goal is to derive the polynomial form of $\boldsymbol{\alpha}(\mathbf{k})$. To this end we note two symmetry properties that can be obtained from Eqs. (10) and (12):

$$\boldsymbol{\alpha}(-\mathbf{k}) = -\boldsymbol{\alpha}(\mathbf{k}), \quad (15)$$

stating that $\alpha_i(k_x, k_y)$ can be expanded in terms of polynomials of odd power, and

$$\boldsymbol{\alpha}(g\mathbf{k}) = \det(g) g \boldsymbol{\alpha}(\mathbf{k}), \quad (16)$$

where $\det(g) = 1$ for proper rotations and $\det(g) = -1$ for improper rotations. Equation (16) is then used to set up linear equations for the coefficients c_i^l of the n th-order polynomials of $\alpha_i(k_x, k_y) = \sum_{l=1, \dots, n} c_i^l k_x^l k_y^{n-l}$ ($i = x, y, z$). Solving this set of linear equations serves to search for the vanishing coefficients, in principle, for any power n , and hence to determine the form of $H_R(\mathbf{k})$.

Another systematic way to obtain $H_R(\mathbf{k})$ relies on the observation that Eq. (16) can be used to formulate the invariance of the Rashba Hamiltonian as

$$H_R(\mathbf{k}) = \boldsymbol{\alpha}(g\mathbf{k}) \cdot [\det(g) g \boldsymbol{\sigma}], \quad (17)$$

also implying that $\boldsymbol{\sigma}$ transforms as an axial vector. Sorting out the components of \mathbf{k} and $\boldsymbol{\sigma}$ according to irreducible representations of $G_{\mathbf{Q}}$, their direct products can again be decomposed into irreducible representations. Equation (17) states that only the total symmetric irreducible representations from this decomposition can contribute to $H_R(\mathbf{k})$. From the corresponding tables of the point groups³³ one can easily construct the possible terms entering $H_R(\mathbf{k})$ according to

TABLE I. Possible terms of the Rashba Hamiltonian for different point groups (first row) containing first-order (second row) and third-order (third row) polynomials of k_x and k_y .

C_{hx}	C_2	C_3	C_4	C_{2v}	C_{3v}	C_{4v}
$k_x\sigma_y,$	$k_x\sigma_x,$	$k_x\sigma_x + k_y\sigma_y,$	$k_x\sigma_x + k_y\sigma_y,$	$k_x\sigma_y,$	$k_x\sigma_y - k_y\sigma_x$	$k_x\sigma_y - k_y\sigma_x$
$k_y\sigma_x,$	$k_x\sigma_y,$	$k_x\sigma_y - k_y\sigma_x$	$k_x\sigma_y - k_y\sigma_x$	$k_y\sigma_x$		
$k_y\sigma_z$	$k_y\sigma_x,$ $k_y\sigma_y$					
$k_x^3\sigma_y,$	$k_x^3\sigma_x,$	$(k_x^3 + k_x k_y^2)\sigma_x +$	$k_x^3\sigma_x + k_y^3\sigma_y,$	$k_x^3\sigma_y,$	$(k_x^3 + k_x k_y^2)\sigma_y -$	$k_x^3\sigma_y - k_y^3\sigma_x,$
$k_x^2 k_y \sigma_x,$	$k_x^3\sigma_y,$	$(k_x^2 k_y + k_y^3)\sigma_y,$	$k_x^3\sigma_y - k_y^3\sigma_x,$	$k_x^2 k_y \sigma_x,$	$(k_x^2 k_y + k_y^3)\sigma_x,$	$k_x^2 k_y \sigma_x - k_x k_y^2 \sigma_y$
$k_x^2 k_y \sigma_z,$	$k_x^2 k_y \sigma_x,$	$(k_x^3 + k_x k_y^2)\sigma_y -$	$k_x^2 k_y \sigma_x - k_x k_y^2 \sigma_y,$	$k_x k_y^2 \sigma_y,$	$(k_x^3 - 3k_x k_y^2)\sigma_z$	
$k_x k_y^2 \sigma_y,$	$k_x^2 k_y \sigma_y,$	$(k_x^2 k_y + k_y^3)\sigma_x,$	$k_x k_y^2 \sigma_x + k_x^2 k_y \sigma_y$	$k_y^3 \sigma_x$		
$k_y^3 \sigma_x,$	$k_x k_y^2 \sigma_x,$	$(k_x^3 - 3k_x k_y^2)\sigma_z,$				
$k_y^3 \sigma_z$	$k_x k_y^2 \sigma_y,$ $k_y^3 \sigma_x,$ $k_y^3 \sigma_y$	$(k_y^3 - 3k_x^2 k_y)\sigma_z$				

increasing powers of k_x and k_y . In the Appendix this procedure is illustrated for the simple case of point group C_{2v} . As one of the main results of this work, in Table I we list the possible terms up to third order in k that can enter $H_R(\mathbf{k})$ for different point groups relevant to surfaces of crystals.

Finally, in this section we comment on the method used in Ref. 35. In this work a Hamiltonian including SOI but excluding all k -dependent terms was considered as the unperturbed system and the twofold degenerate solutions ϕ_1 and ϕ_2 , corresponding to the wave number \mathbf{Q} as the unperturbed solutions. The perturbation was therefore taken as $\mathcal{H}'(\mathbf{k}) = \frac{\hbar}{m} \mathbf{k} \mathbf{p} + \frac{\hbar^2}{4m^2 c^2} (\nabla \mathbf{V} \times \mathbf{k}) \cdot \boldsymbol{\sigma}$ and, similar to our strategy, first-order degenerate perturbation theory was applied. The form of the effective Rashba Hamiltonian, $H'_{ij}(\mathbf{k}) = \langle \phi_i | \mathcal{H}'(\mathbf{k}) | \phi_j \rangle$ ($i, j = 1, 2$), is then determined via the invariance conditions,

$$H'(g\mathbf{k}) = D(g) H'(\mathbf{k}) D(g)^{-1}, \quad (18)$$

where $D(g)$ is a 2×2 unitary double-point-group representation of g . In the case of Abelian point groups (C_{hx} , C_2 , C_3 , and C_4), the degenerate states form time-reversed pairs and $D(g)$ can simply be set up from the characters of the corresponding one-dimensional irreducible representations. Following from the definition of $H'(\mathbf{k})$, in Ref. 35 the first-order Rashba Hamiltonians were obtained for the groups C_{hx} , C_{2v} , C_{3v} , and C_{4v} . It is, however, straightforward to show that when applied to the Hamiltonian (13), Eq. (18) is equivalent with condition (17);³⁹ hence using double-group representations leads to the same results as listed in Table I.

III. THIRD-ORDER RASHBA SPLITTING AT Bi/Ag(111)

By using the screened Korringa-Kohn-Rostoker (KKR) method⁴⁰ we performed calculations for the $(\sqrt{3} \times \sqrt{3})R30^\circ$ ordered surface alloy Bi/Ag(111) to obtain a quantitative verification of our prediction of a third-order Rashba Hamiltonian. A 2D lattice constant of 2.892 Å related to fcc Ag bulk and, according to geometry optimization we performed in terms of

the VASP method⁴¹ and also in agreement with previous LAPW calculations,¹⁹ an outward buckling of 36% (0.85 Å) for the Bi atoms was considered. In accordance with the concept of perturbation theory, we performed self-consistent calculations within the scalar-relativistic approach, while we included SOI only when calculating the dispersion relation of the surface states. The local spin-density approximation as parametrized by Vosko *et al.*⁴² was applied, and the effective potentials and fields were treated within the atomic sphere approximation (ASA) with an angular momentum cut-off of $\ell_{\max} = 2$. For a better positioning of the surface states with respect to the Fermi energy, we determined the Fermi level of bulk Ag by using $\ell_{\max} = 3$. The energy integrations were performed by sampling 12 points on a semicircular path in the upper complex semiplane, and for the necessary k integrations we selected 36 k points in the irreducible segment of the surface Brillouin zone.

As is well-known, ASA gives a rather poor description of the surface potential barrier, pushing, in general, the surface states to significantly low binding energies. In order to cure this problem, the positions of the empty-sphere layers are usually relaxed in appropriate amounts.⁴³ Probably due to the large relaxation of the Bi atoms, in the present case, this procedure was not successful in getting reliable binding energies. According to our experience, the main reason for this deficiency was the very low value of the Madelung potential for the empty spheres adjacent to the Ag_2Bi surface layer. Shifting this potential up artificially by about 0.5 Ry (near to that of the constant vacuum potential) indeed resulted in an upward shift of the Bi surface states close to the energy region comparable to the experiment. Nevertheless, we should emphasize that the first-principles calculations we present now serve for illustrating the predictions of the perturbation theory presented in Sec. II rather than for providing a precise comparison to experiment.

The calculated dispersion relations of the Bi surface states are shown in Fig. 1 along the $\bar{\Gamma}\bar{M}$ direction of the SBZ. As

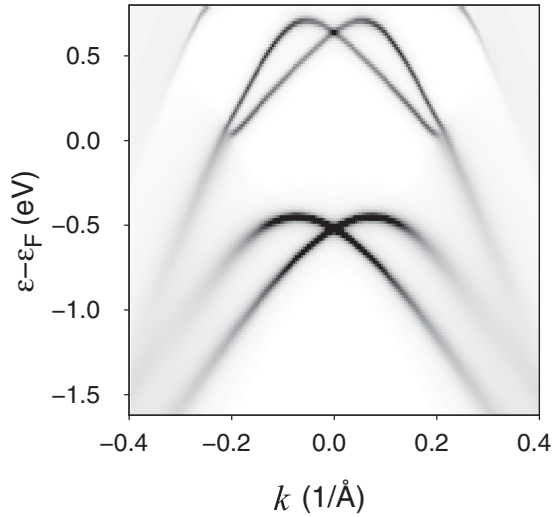


FIG. 1. Calculated dispersion relations of the surface states of Bi/Ag(111) along the $\bar{\Gamma}\bar{M}$ direction of the SBZ. Lower branches: sp_z states, upper branches: p_x, p_y states.

explained above, we managed to place the occupied sp_z band by only 0.3 and 0.1 eV lower in binding energy as compared to the experiment and a previous KKR calculation,¹⁸ respectively. Consequently, the position and also the shape of the mainly unoccupied Bi p_x, p_y surface band agree well with those from similar first-principles calculations.²² Particular features of this band, namely, a large deviation from a parabolic shape and a visual merging of the Rashba-split branches for $k > 0.2 \text{ \AA}^{-1}$, imply highly anisotropic effects that, most probably, go beyond the validity of perturbation theory. Therefore in what follows we deal only with the analysis of the occupied surface states. The maxima of the Bi sp_z band are shifted from the $\bar{\Gamma}$ point by $k_0 = 0.1 \text{ \AA}^{-1}$ and, using a parabolic fit around the maxima, we obtained an effective mass of $m^* = -0.36 m_e$. These values are in reasonably good agreement with experimental data, $k_0 = 0.13 \text{ \AA}^{-1}$ and $m^* = -0.35 m_e$.¹⁸

In the case of C_{3v} symmetry the effective Rashba Hamiltonian can be written up to third order in k as (see Table I),

$$H_R(\underline{k}) = (\alpha_1 k + \alpha_3^1 k^3)(\cos \varphi \sigma_y - \sin \varphi \sigma_x) + \alpha_3^2 k^3 \cos 3\varphi \sigma_z, \quad (19)$$

with the polar coordinate $\varphi = \arccos(k_x/k)$. Note that the x axis was chosen along the $\bar{\Gamma} - \bar{K}$ direction of the SBZ. Obviously, there are two kinds of third-order contributions to the Hamiltonian (19): an isotropic one with coefficient α_3^1 and an anisotropic one with the coefficient α_3^2 . The square of the splitting of the eigenvalues, $\Delta\epsilon(\mathbf{k}) = [\epsilon_+(\mathbf{k}) - \epsilon_-(\mathbf{k})]/2$, can then be expressed as

$$\Delta\epsilon(\mathbf{k})^2 = (\alpha_1 k + \alpha_3^1 k^3)^2 + (\alpha_3^2)^2 k^6 \cos^2 3\varphi. \quad (20)$$

In Fig. 2 we plotted $\Delta\epsilon(\mathbf{k})^2$ along the $\bar{\Gamma}\bar{K}$ and the $\bar{\Gamma}\bar{M}$ directions, together with different fitting functions related to Eq. (20). It can be seen that a parabolic fit (dots), $\alpha_1 k^2$ with $\alpha_1 = 1.74 \text{ eV \AA}$, applies well to the two curves only for about $k < 0.07 \text{ \AA}^{-1}$. Up to $k \sim 0.13 \text{ \AA}^{-1}$ the two curves still coincide; however, the isotropic third-order contribution is needed for a good fit. Here we used a fitting function

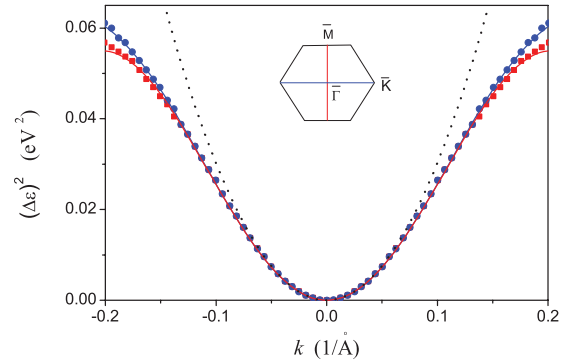


FIG. 2. (Color online) Square of the calculated splitting $\Delta\epsilon(\mathbf{k}) = [\epsilon_+(\mathbf{k}) - \epsilon_-(\mathbf{k})]/2$ of the occupied surface states of Bi/Ag(111). Squares: $\bar{\Gamma}\bar{M}$ direction, circles: $\bar{\Gamma}\bar{K}$ direction (see the sketch of the SBZ in the inset). Dotted and solid lines display first-order and third-order fits as described in the text.

$(\alpha_1 k + \alpha_3^1 k^3)^2$ with the same value for α_1 as before and $\alpha_3^1 = -14.2 \text{ eV \AA}^3$. For wave numbers $k > 0.13 \text{ \AA}^{-1}$, the anisotropy of the RB splitting becomes apparent: along $\bar{\Gamma}\bar{M}$ ($\varphi = \pi/2$) the previous fit applies, while along $\bar{\Gamma}\bar{K}$ ($\varphi = 0$) the fitting function had to be extended by the anisotropic term, $(\alpha_3^2)^2 k^6$ with $\alpha_3^2 = 9.4 \text{ eV \AA}^3$.

It is worthwhile to mention here that the parameters fitted in Ref. 38 to the occupied surface band of Bi/Ag(111), $\alpha_1 = 2.95 \text{ eV \AA}$ and $\alpha_3^2 = 18 \text{ eV \AA}^3$, show remarkable differences as compared to our fitted values. On the one hand, this can be understood that in Ref. 38 constant-energy contours related to experiments and first-principles calculations^{18,44} were used for fitting. On the other hand, it should be emphasized that the fit of Ref. 38 disregarded the isotropic third-order term $\alpha_3^1 k^3$ in the Rashba Hamiltonian (19). In contrast, our numerical results clearly support the appearance of both the isotropic and the anisotropic third-order terms for the Bi sp_z surface states of Bi/Ag(111), consistent with the functional form as derived from group-theoretical methods.

IV. COMPARISON OF THE RASHBA EFFECT AT Au(111) AND Bi/Ag(111)

It is well known from experiments and *ab initio* calculations^{1,3-6} that the Au(111) L -gap surface states show a highly isotropic (first-order) Rashba splitting. Since both systems, Au(111) and Bi/Ag(111), exhibit C_{3v} symmetry, the question naturally arises as to why there is a remarkable difference concerning third-order RB splitting. In order to find, at least, a qualitative understanding of the problem, we extended the $k \cdot p$ perturbation calculations presented in Ref. 10 for the case of C_{2v} symmetry to C_{3v} symmetry and found the following expressions for the third-order coefficients in Eq. (19):

$$\alpha_3^1 = \frac{\hbar^4}{4m^4 c^2} \sum_{n,m} \frac{\langle \phi_0 | p_x | \phi_n^+ \rangle \langle \phi_n^+ | \partial_z V | \phi_m^+ \rangle \langle \phi_m^+ | p_x | \phi_0 \rangle}{(\epsilon_0 - \epsilon_n^E)(\epsilon_0 - \epsilon_m^E)} \quad (21)$$

and

$$\alpha_3^2 = \frac{\hbar^4}{4m^4c^2} \sum_{n,m} \frac{\langle \phi_0 | p_x | \phi_n^+ \rangle \langle \phi_n^+ | \partial_x V | \phi_m^- \rangle \langle \phi_m^- | p_x | \phi_0 \rangle}{(\varepsilon_0 - \varepsilon_n^E)(\varepsilon_0 - \varepsilon_m^E)}. \quad (22)$$

From the above formulas it turns out that third-order corrections to the effective Hamiltonian arise from an admixture between the surface state, ϕ_0 of sp_z orbital character at energy ε_0 , and those corresponding to the two-dimensional irreducible representation, E , ϕ_n^\pm with $p_x \pm ip_y$ character, at energy ε_n^E . Note that all these states are eigenstates of the Hamiltonian $\mathcal{H} = \frac{p^2}{2m} + V$ at the center of the surface band \mathbf{Q} . It is remarkable that, similar to the isotropic first-order Rashba parameter, the strength of the isotropic contribution α_3^1 depends on the partial derivative of the crystal potential normal to the surface $\partial_z V$, while the coefficient for the anisotropic term α_3^2 is related to the in-plane gradient of the potential $\partial_x V$.

In Fig. 3 we plotted the scalar-relativistic, orbital projected densities of states (Bloch spectral functions) at the $\bar{\Gamma}$ point in an appropriate energy window around the surface states of Au(111) and Bi/Ag(111). In case of Au(111) (see the upper panel of Fig. 3) the localized surface state shows up in a sharp peak near the Fermi level ($\varepsilon_0 \simeq -0.07$ eV), while the bulk bands are located below -1 eV. In particular, the edge of the bulk subband of E symmetry (d_{xz}, d_{yz} states) closest to the surface state is by $\Delta\varepsilon = 1.77$ eV below ε_0 .

The situation is entirely different for Bi/Ag(111), where the highly localized Bi sp_z and $p_x p_y$ states are far in energy from the bulk states. Since in this case only the Bi $p_x p_y$ states of E symmetry contribute to Eqs. (21) and (22), $\Delta\varepsilon = 0.27$ eV enters the corresponding denominators. This clearly explains a difference of at least 2 orders in magnitude concerning the third-order RB effect of Au(111) and Bi/Ag(111). Most probably, the actual values of the matrix elements of p_x and $\partial_{x,z} V$ even further strengthen this difference. Contrasting the $k = 0$ cut of Fig. 1 with the lower panel of Fig. 3, it is remarkable that the spin-degenerate sp_z states are shifted down by about 1 eV due to SOI, while the fourfold degenerate $p_x p_y$ states are split into two parts according to the two-dimensional double-group representations: one of them is located at 0.6 eV, the other one is moved up to 1.21 eV (not shown in Fig. 1).

V. CONCLUSIONS

Based on $k \cdot p$ perturbation theory including spin-orbit interaction, we gave a suitable definition to an effective Hamiltonian [Eqs. (13) and (14)] describing the Rashba-Bychkov splitting on metallic surfaces. Due to time reversal and point-group symmetry, we showed how to obtain the most general forms for the effective Hamiltonian and derived them up to third order in k for point groups compatible with surfaces of real crystals. Since the effective Hamiltonian (13) applies to a couple of noninteracting two-band models, the expressions listed in Table I can be used in quite a general sense.

Using the relativistic screened Korringa-Kohn-Rostoker method, we demonstrated that the Rashba splitting of the Bi sp_z surface band of the ordered surface alloy Bi/Ag(111) cannot be satisfactorily described in terms of a first-order isotropic Rashba Hamiltonian. Moreover, we showed that the strong

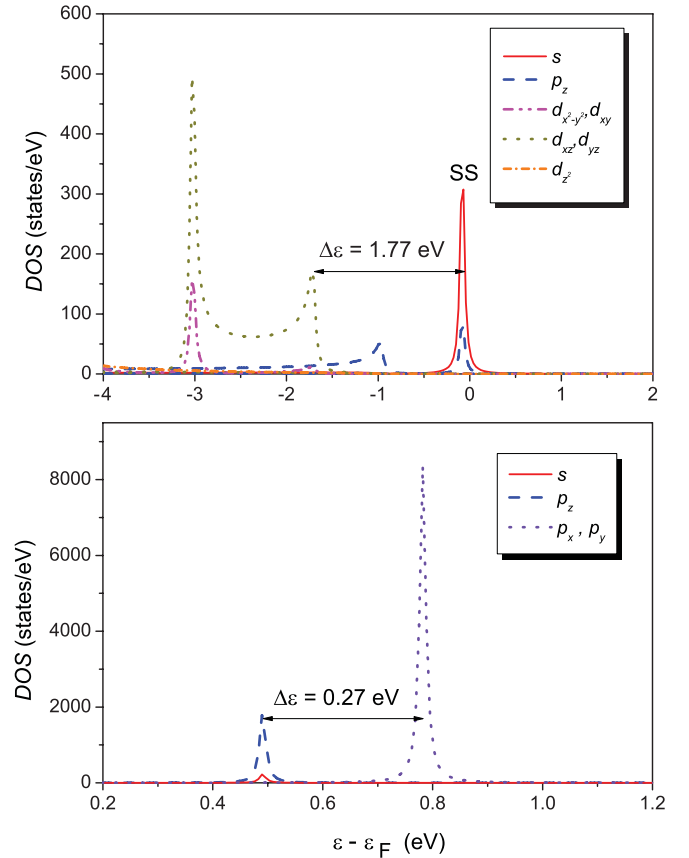


FIG. 3. (Color online) Calculated scalar-relativistic orbital projected spectral densities of states at the $\bar{\Gamma}$ point of Au(111) (upper panel) and Bi/Ag(111) (lower panel). The surface state (SS) of Au(111) is explicitly labeled. For Bi/Ag(111) only the two localized Bi states are shown that take place in the L-gap of Ag(111).

third-order contribution is subject to an anisotropy consistent with the dispersion relation deduced from our symmetry analysis.

We also derived explicit formulas for the third-order anisotropy parameters and established that the isotropic and anisotropic contributions are related to the normal-to-plane and the in-plane gradients of the crystal potential, respectively. Comparing the energy separation of relevant orbital projected bands for Au(111) and Bi/Ag(111), the derived expressions were useful to give a qualitative understanding of the different nature of Rashba-Bychkov splitting in these two systems.

ACKNOWLEDGMENTS

The authors appreciate stimulating discussions with Gergely Zarand. Financial support was provided by the Hungarian Research Foundation (Contracts No. OTKA K77771, OTKA K84078, and OTKA PD83353) and by the New Széchenyi Plan of Hungary (Project ID: TÁMOP-4.2.1/B-09/1/KMR-2010-0002). K.P. kindly acknowledges support from a Bolyai Grant.

**APPENDIX: RASHBA HAMILTONIANS
FOR POINT GROUP C_{2v}**

By using the direct products of irreducible representations, in this Appendix we give an example for the polynomial forms of a 2×2 effective Hamiltonian for the point group C_{2v} . Let us denote the elements of the group by $E : \{x, y, z\}$, $C_2 : \{-x, -y, z\}$, $S_x : \{-x, y, z\}$, and $S_y : \{x, -y, z\}$. The group has four one-dimensional irreducible representations, A_1 , A_2 , B_1 , and B_2 , with the character table³³

	E	C_2	S_x	S_y
A_1	1	1	1	1
A_2	1	1	-1	-1
B_1	1	-1	-1	1
B_2	1	-1	1	-1

Since \mathbf{k} and $\boldsymbol{\sigma}$ are transformed as polar and axial vectors, respectively, a comparison with the character table lets us sort out the components of these vectors according to irreducible representations: $B_1 : k_x, \sigma_y$, $B_2 : k_y, \sigma_x$, and $A_2 : \sigma_z$.

From the table of direct products,

	A_1	A_2	B_1	B_2
A_1	A_1	A_2	B_1	B_2
A_2		A_1	B_2	B_1
B_1			A_1	A_2
B_2				A_1

it is easy to find that the only combinations that are first order in k_x and k_y and correspond to the A_1 irreducible representations are $k_x \sigma_y$ and $k_y \sigma_x$; therefore the first-order Rashba Hamiltonian can be written in the form of Eq. (2).

The second-order polynomials of k_x and k_y can be sorted according to irreducible representations as follows: $A_1 : k_x^2, k_y^2$ and $A_2 : k_x k_y$. It should be noted that this implies the form of $\frac{\hbar^2}{2m_x^*} k_x^2 + \frac{\hbar^2}{2m_y^*} k_y^2$ for the effective mass term. The third-order polynomials of k_x and k_y can then be classified as $B_1 : k_x^3, k_x k_y^2$ and $B_2 : k_y^3, k_y k_x^2$. Taking direct products with σ_i of A_1 symmetry leads to the possible third-order contributions to the Rashba Hamiltonian: $k_x^3 \sigma_y, k_x^2 k_y \sigma_x, k_x k_y^2 \sigma_y$, and $k_y^3 \sigma_x$, i.e.,

$$H_{R,3}(\mathbf{k}) = \alpha_3^1 k_x^3 \sigma_y + \alpha_3^2 k_x^2 k_y \sigma_x + \alpha_3^3 k_x k_y^2 \sigma_y + \alpha_3^4 k_y^3 \sigma_x. \quad (\text{A1})$$

*szunyogh@phy.bme.hu

¹S. LaShell, B. A. McDougall, and E. Jensen, *Phys. Rev. Lett.* **77**, 3419 (1996).

²Y. A. Bychkov and E. I. Rashba, *J. Phys. C* **17**, 6039 (1984).

³G. Nicolay, F. Reinert, S. Hüfner, and P. Blaha, *Phys. Rev. B* **65**, 033407 (2001).

⁴J. Henk, A. Ernst, and P. Bruno, *Phys. Rev. B* **68**, 165416 (2003).

⁵J. Henk, M. Hoesch, J. Osterwalder, A. Ernst, and P. Bruno, *J. Phys. Condens. Matter* **16**, 7581 (2004).

⁶R. Mazzarello, A. Dal Corso, and E. Tosatti, *Surf. Sci.* **602**, 803 (2008).

⁷A. Nuber, J. Braun, F. Forster, J. Minár, F. Reinert, and H. Ebert, *Phys. Rev. B* **83**, 165401 (2011).

⁸A. Nuber, M. Higashiguchi, F. Forster, P. Blaha, K. Shimada, and F. Reinert, *Phys. Rev. B* **78**, 195412 (2008).

⁹M. Nagano, A. Kodama, T. Shishidou, and T. Oguchi, *J. Phys. Condens. Matter* **21**, 064239 (2009).

¹⁰E. Simon, A. Szilva, B. Ujjfalussy, B. Lazarovits, G. Zarand, and L. Szunyogh, *Phys. Rev. B* **81**, 235438 (2010).

¹¹E. Rotenberg, J. W. Chung, and S. D. Kevan, *Phys. Rev. Lett.* **82**, 4066 (1999).

¹²O. Krupin, G. Bihlmayer, K. Starke, S. Gorovikov, J. E. Prieto, K. Döbrich, S. Blügel, and G. Kaindl, *Phys. Rev. B* **71**, 201403 (2005).

¹³Yu. M. Koroteev, G. Bihlmayer, J. E. Gayone, E. V. Chulkov, S. Blügel, P. M. Echenique, and Ph. Hofmann, *Phys. Rev. Lett.* **93**, 046403 (2004).

¹⁴Ph. Hofmann, J. E. Gayone, G. Bihlmayer, Yu. M. Koroteev, and E. V. Chulkov, *Phys. Rev. B* **71**, 195413 (2005).

¹⁵K. Sugawara, T. Sato, S. Souma, T. Takahashi, M. Arai, and T. Sasaki, *Phys. Rev. Lett.* **96**, 046411 (2006).

¹⁶T. Hirahara, T. Nagao, I. Matsuda, G. Bihlmayer, E. V. Chulkov, Yu. M. Koroteev, P. M. Echenique, M. Saito, and S. Hasegawa, *Phys. Rev. Lett.* **97**, 146803 (2006).

¹⁷D. Pacilé, C. R. Ast, M. Papagno, C. Da Silva, L. Moreschini, M. Falub, A. P. Seitsonen, and M. Grioni, *Phys. Rev. B* **73**, 245429 (2006).

¹⁸C. R. Ast, J. Henk, A. Ernst, L. Moreschini, M. C. Falub, D. Pacilé, P. Bruno, Kl. Kern, and M. Grioni, *Phys. Rev. Lett.* **98**, 186807 (2007).

¹⁹G. Bihlmayer, S. Blügel, and E. V. Chulkov, *Phys. Rev. B* **75**, 195414 (2007).

²⁰C. R. Ast, G. Wittich, P. Wahl, R. Vogelgesang, D. Pacilé, M. C. Falub, L. Moreschini, M. Papagno, M. Grioni, and K. Kern, *Phys. Rev. B* **75**, 201401(R) (2007).

²¹J. H. Dil, F. Meier, J. Lobo-Checa, L. Patthey, G. Bihlmayer, and J. Osterwalder, *Phys. Rev. Lett.* **101**, 266802 (2008).

²²C. R. Ast, D. Pacilé, L. Moreschini, M. C. Falub, M. Papagno, K. Kern, M. Grioni, J. Henk, A. Ernst, S. Ostanin, and P. Bruno, *Phys. Rev. B* **77**, 081407(R) (2008).

²³T. Hirahara, T. Komorida, A. Sato, G. Bihlmayer, E. V. Chulkov, K. He, I. Matsuda, and S. Hasegawa, *Phys. Rev. B* **78**, 035408 (2008).

²⁴L. Moreschini, A. Bendounan, I. Gierz, C. R. Ast, H. Mirhosseini, H. Höchst, K. Kern, J. Henk, A. Ernst, S. Ostanin, F. Reinert, and M. Grioni, *Phys. Rev. B* **79**, 075424 (2009).

²⁵L. Moreschini, A. Bendounan, H. Bentmann, M. Assig, K. Kern, F. Reinert, J. Henk, C. R. Ast, and M. Grioni, *Phys. Rev. B* **80**, 035438 (2009).

²⁶I. Gierz, B. Stadtmüller, J. Vuorinen, M. Lindroos, F. Meier, J. H. Dil, K. Kern, and C. R. Ast, *Phys. Rev. B* **81**, 245430 (2010).

- ²⁷H. Mirhosseini, I. V. Maznichenko, S. Abdelouahed, S. Ostanin, A. Ernst, I. Mertig, and J. Henk, *Phys. Rev. B* **81**, 073406 (2010).
- ²⁸S. Abdelouahed and J. Henk, *Phys. Rev. B* **82**, 193411 (2010).
- ²⁹For a review, see I. Zutic, J. Fabian, and S. Das Sarma, *Rev. Mod. Phys.* **76**, 323 (2004).
- ³⁰J. Sinova, D. Culcer, Q. Niu, N. A. Sinitsyn, T. Jungwirth, and A. H. MacDonald, *Phys. Rev. Lett.* **92**, 126603 (2004); J. Wunderlich, B. Kaestner, J. Sinova, and T. Jungwirth, *ibid.* **94**, 047204 (2005).
- ³¹D. Culcer, A. MacDonald, and Q. Niu, *Phys. Rev. B* **68**, 045327 (2003); V. K. Dugaev, P. Bruno, M. Taillefumier, B. Canals, and C. Lacroix, *ibid.* **71**, 224423 (2005); T. S. Nunner, G. Zarand, and F. von Oppen, *Phys. Rev. Lett.* **100**, 236602 (2008).
- ³²L. Petersen and P. Hedegård, *Surf. Sci.* **459**, 49 (2000).
- ³³In this work we use the standard Schönflies notations for point groups, see S. L. Altmann and P. Herzig, *Point-Group Theory Tables* (Clarendon Press, Oxford, 1984).
- ³⁴J. Prempfer, M. Trautmann, J. Henk, and P. Bruno, *Phys. Rev. B* **76**, 073310 (2007).
- ³⁵T. Oguchi and T. Shishidou, *J. Phys.: Condens. Matter* **21**, 092001 (2009).
- ³⁶L. Fu, *Phys. Rev. Lett.* **103**, 266801 (2009).
- ³⁷Y. L. Chen, J. G. Analytis, J.-H. Chu, Z. K. Liu, S.-K. Mo, X. L. Qi, H. J. Zhang, D. H. Lu, X. Dai, Z. Fang, S. C. Zhang, I. R. Fisher, Z. Hussain, and Z.-X. Shen, *Science* **325**, 178 (2009).
- ³⁸E. Frantzeskakis and M. Grioni, *Phys. Rev. B* **84**, 155453 (2011).
- ³⁹Sz. Vajna, B.Sc. thesis, Budapest University of Technology and Economics (2010).
- ⁴⁰J. Zablouil, R. Hammerling, L. Szunyogh, and P. Weinberger, *Electron Scattering in Solid Matter: A Theoretical and Computational Treatise* (Springer, Berlin, 2005).
- ⁴¹G. Kresse and J. Hafner, *Phys. Rev. B* **47**, 558 (1993); **49**, 14251 (1994); G. Kresse and J. Furthmüller, *Comput. Mater. Sci.* **6**, 15 (1996); **54**, 11169 (1996).
- ⁴²S. H. Vosko, L. Wilk, and M. Nusair, *Can. J. Phys.* **58**, 1200 (1980).
- ⁴³J. Henk, M. Hoesch, J. Osterwalder, A. Ernst, and P. Bruno, *J. Phys.: Condens. Matter* **16**, 7581 (2004).
- ⁴⁴H. Bentmann, F. Forster, G. Bihlmayer, E. V. Chulkov, L. Moreschini, M. Grioni, and F. Reinert, *Europhys. Lett.* **87**, 37003 (2009).